

# Targeting Ribosome Biogenesis for Cancer Therapy with Oral Platinum Complexes

Dongfan Song,<sup>§</sup> Xiaoyu Wang,<sup>§</sup> Zihan Zhao,<sup>§</sup> Rong Yang, Shuren Zhang,\* and Zijian Guo\*



Cite This: *JACS Au* 2025, 5, 73–81



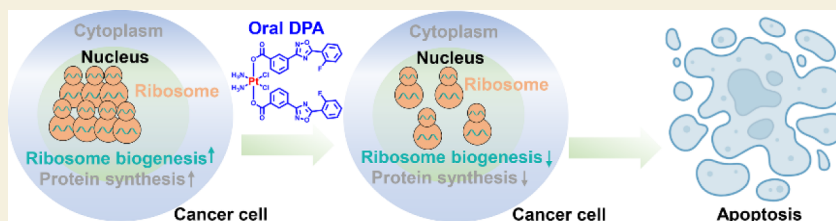
Read Online

ACCESS |

Metrics & More

Article Recommendations

Supporting Information



**ABSTRACT:** Cancer cells often upregulate ribosome biogenesis to meet increased protein synthesis demands for rapid proliferation; therefore, targeting ribosome biogenesis has emerged as a promising cancer therapeutic strategy. Herein, we introduce two Pt complexes, ataluren monosubstituted platinum(IV) (SPA, formula:  $c,c,t$ -[Pt(NH<sub>3</sub>)<sub>2</sub>Cl<sub>2</sub>(OH)(C<sub>15</sub>H<sub>8</sub>FN<sub>2</sub>O<sub>3</sub>)], where C<sub>15</sub>H<sub>8</sub>FN<sub>2</sub>O<sub>3</sub> = ataluren) and ataluren bisubstituted platinum(IV) complex (DPA, formula:  $c,c,t$ -[Pt(NH<sub>3</sub>)<sub>2</sub>Cl<sub>2</sub>(C<sub>15</sub>H<sub>8</sub>FN<sub>2</sub>O<sub>3</sub>)<sub>2</sub>], where C<sub>15</sub>H<sub>8</sub>FN<sub>2</sub>O<sub>3</sub> = ataluren), which effectively suppress ribosome biogenesis by inhibiting 47s pre-RNA expression. Furthermore, SPA and DPA induce nucleolar stress by dispersing nucleolar protein NPM1, ultimately inhibiting protein generation in tumor cells. More importantly, DPA exhibits superior cytotoxicity to various cancer cells and *in vivo* antitumor efficacy compared to cisplatin, with lower systemic toxicity. Notably, in clinically relevant models, including orthotopic hepatic tumor-bearing mice and patient-derived bladder cancer organoids, DPA outperforms cisplatin significantly, with the added benefit of oral administration, enhancing clinical feasibility. To our knowledge, DPA emerges as the pioneering Pt(IV) agent targeting the ribosome, providing new insights for designing next-generation metal-based therapeutics.

**KEYWORDS:** anticancer drug, ribosome biogenesis, oral drug, platinum drug, patient-derived tumor organoid

## INTRODUCTION

Ribosomes are essential cellular organelles responsible for protein synthesis. The biogenesis of ribosomes is a complex and tightly regulated process involving the transcription, processing, and assembly of ribosomal RNA (rRNA) with ribosomal proteins.<sup>1,2</sup> Dysregulation of ribosome biogenesis has been implicated in various diseases, including cancer. In cancer cells, ribosome biogenesis is often upregulated to meet the increased demand for protein synthesis required for their rapid proliferation.<sup>3,4</sup> Therefore, targeting ribosome biogenesis has emerged as a promising strategy for cancer therapy.

DNA-damaging agents, such as chemotherapy and radiation therapy, can induce increased instability of ribosomal DNA (rDNA) by causing DNA lesions and triggering DNA repair mechanisms.<sup>5,6</sup> This increased rDNA instability can lead to aberrant rRNA synthesis and ribosome biogenesis. This, in turn, can cause interruptions in protein synthesis and changes in ribosome function, ultimately leading to cellular stress and potentially affecting cell viability.<sup>7</sup> Platinum (Pt)-based drugs, such as cisplatin (CDDP), carboplatin and oxaliplatin, are widely used DNA-damaging agents in cancer therapy.<sup>8,9</sup> These drugs form DNA adducts that induce DNA damage and activate cellular stress responses.<sup>10</sup> Interestingly, oxaliplatin and its

derivatives have been reported to kill cancer cells by inducing ribosome biogenesis stress and nucleolar stress,<sup>11,12</sup> while CDDP can intercalate between the ribosome and mRNA, potentially affecting protein synthesis and ribosomal function.<sup>13,14</sup> These findings suggest that Pt complexes represent a potent class of inhibitors targeting ribosome biogenesis.

The effectiveness of traditional Pt(II) drugs is often limited by the development of drug resistance and associated toxicities.<sup>15</sup> Pt(IV) complexes have emerged as a promising class of antitumor compounds due to their unique chemical properties and favorable pharmacological profiles.<sup>16</sup> These complexes remain stable in the bloodstream and normal tissues but become active within cancer cells upon reduction to Pt(II) species, along with the release of axial ligands.<sup>17</sup> The inertness of Pt(IV) complexes minimizes unwanted interactions with nucleophiles in the serum, reducing side effects, and can be administered

**Received:** July 18, 2024

**Revised:** November 7, 2024

**Accepted:** November 8, 2024

**Published:** December 17, 2024



orally.<sup>18</sup> Satraplatin completed Phase III clinical trials via oral administration but was not approved due to no significant improvement in overall survival. However, it significantly increased progression-free survival, highlighting the oral efficacy of Pt(IV) compounds.<sup>19</sup> Through Pt(IV) prodrug platform, a diverse array of multifunctional, multitargeted and highly potent compounds has been developed.<sup>18,20–25</sup> Yet, the design of Pt(IV) drugs targeting the ribosome still represents a nascent frontier in research.

In this context, we have used a Pt(IV) prodrug strategy to develop two novel Pt compounds, SPA and DPA, and with the axial ligand Ataluren (Ata) (see Figure 1). Ata is thought to

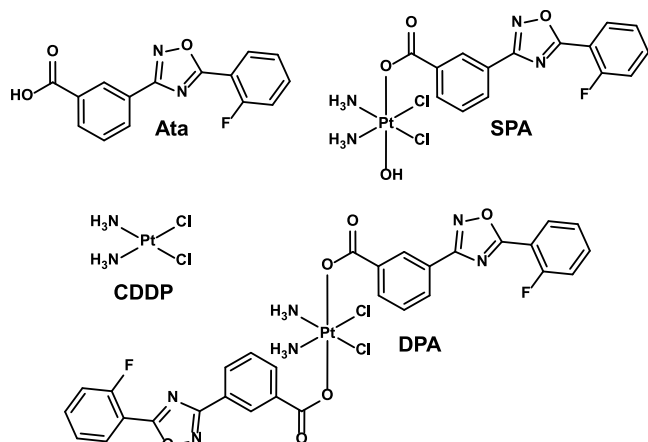


Figure 1. Chemical structures of CDDP, Ata, SPA, and DPA.

modulate ribosome to promote therapeutic nonsense suppression and has been approved in the European Union for the treatment of nonsense mutation Duchenne muscular dystrophy.<sup>26–28</sup> Our research indicates that DPA exhibits the ability to inhibit ribosome biogenesis and protein synthesis. Remarkably, it demonstrated oral bioavailability and exhibit

outstanding efficacy in an orthotopic liver tumors-bearing mice and patient-derived bladder cancer organoids.

## RESULTS AND DISCUSSION

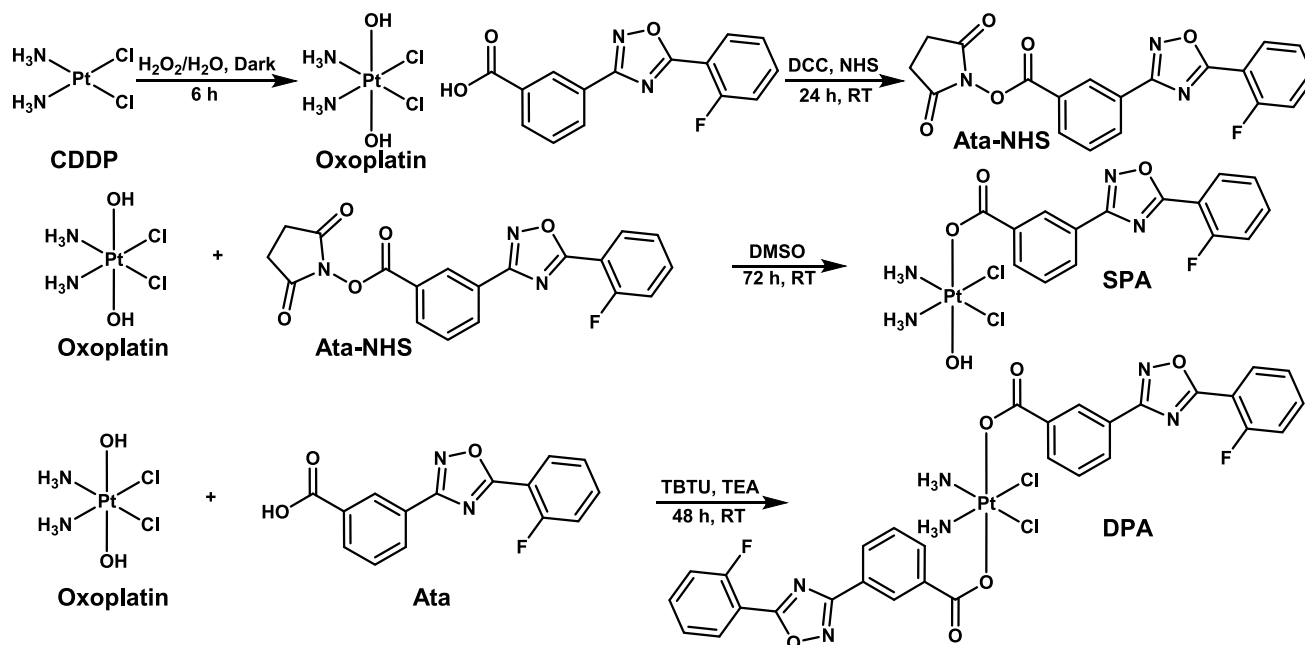
### Synthesis and Characterization

Scheme 1 illustrates the synthetic routes to SPA and DPA. These complexes were synthesized using a previously documented procedure.<sup>29</sup> Initially, the Pt(IV) intermediate, oxoplatin, was synthesized via the oxidation of CDDP with hydrogen peroxide ( $\text{H}_2\text{O}_2$ ). Subsequently, Ata-NHS ester was prepared as per established protocols in the literature.<sup>30</sup> SPA and DPA were synthesized by reacting Ata-NHS and Ata with oxoplatin, respectively. The structural integrity of SPA and DPA was confirmed through various analytical techniques, including  $^1\text{H}$ -,  $^{13}\text{C}$ -, and  $^{195}\text{Pt}$ -NMR, as well as high-resolution mass spectra (refer to Figures S1–S8). Notably, the  $^{195}\text{Pt}$ -NMR spectra exhibited resonance peaks at  $\delta$  1035.63 and 1156.53 ppm, confirming the presence of Pt(IV) in SPA and DPA, respectively. Moreover, the purity of the complexes was assessed using high-performance liquid chromatography (HPLC) (refer to Figure S9). Considering the necessity of oral administration for Pt(IV) compounds, we assessed the stability of SPA and DPA in artificial gastric and intestinal fluids. After a 24-h incubation period, SPA demonstrated stability in both artificial gastric and intestinal fluids. In contrast, DPA maintained stability in artificial gastric fluid, while over 70% of the compound remained stable in artificial intestinal fluid (Figures S10 and S11). These results highlight their potential suitability for oral delivery.

### Reduction of SPA and DPA

The reduction of Pt(IV) complexes is pivotal for their antitumor efficacy.<sup>31</sup> Cellular reductants like ascorbic acid (AsA) commonly facilitate this reduction, resulting in the release of Pt(II) species along with axial ligands. To assess the reducibility of SPA and DPA, these complexes underwent incubation with excess AsA (8 equiv) individually and were monitored via  $^1\text{H}$

### Scheme 1. Synthetic Routes to SPA and DPA



NMR. As depicted in Figures 2, S10, and S11, the peak corresponding to SPA and DPA gradually diminished over time,

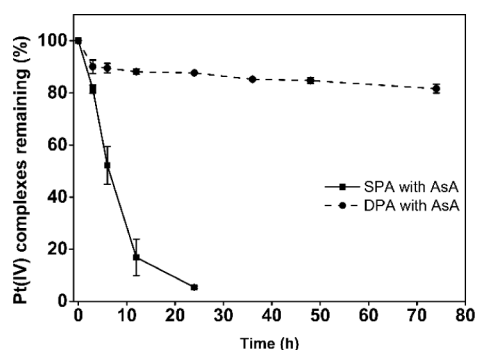


**Figure 2.** Remaining Pt(IV) complexes after the reaction of SPA and DPA with AsA at 37 °C in the dark.

while new peaks reminiscent of the Ata peak emerged, indicating the liberation of axial ligands under reducing conditions. Notably, SPA exhibited a more rapid reduction rate compared to DPA.

### Cytotoxicity of SPA and DPA

The cytotoxicity of the compounds was assessed using the MTT assay across various human cancer cell lines, including MCF-7 (breast cancer), Caov3 (CDDP-insensitive ovarian cancer), and U87MG (glioma). Table 1 lists the half maximal inhibitory

**Table 1.** IC<sub>50</sub> [μM] of SPA, DPA, CDDP, Oxoplatin, Ata and CDDP Plus Ata (1:1 and 1:2) at 72 h against Different Cell Lines<sup>a</sup>

Complex	MCF-7	Caov3	U87MG
SPA	1.92 ± 0.34	2.83 ± 0.77	1.72 ± 0.21
DPA	0.72 ± 0.26	0.98 ± 0.33	0.43 ± 0.05
CDDP	3.59 ± 0.59	21.24 ± 2.91	6.06 ± 0.74
CDDP + Ata	5.03 ± 0.37	20.47 ± 2.77	7.79 ± 0.47
CDDP + 2Ata	4.39 ± 0.23	21.86 ± 0.68	8.07 ± 0.47
oxoplatin	13.27 ± 0.48	>50	24.56 ± 1.85
Ata	>50	>50	>50

<sup>a</sup>Data are average of 3 parallel tests.

concentrations (IC<sub>50</sub>) of the compounds against these cell lines after 72 h. Both SPA and DPA displayed superior activity compared to CDDP across all tested cell lines, irrespective of their sensitivity or resistance to platinum. Ata exhibited negligible cytotoxicity below 50 μM. Mixtures of CDDP and Ata at ratios of 1:1 or 1:2 showed cytotoxicity levels comparable to, or slightly lower than, CDDP, while oxoplatin demonstrated significantly reduced cytotoxicity. Notably, DPA exhibited markedly higher cytotoxicity than SPA across all tested cell lines, warranting further mechanistic investigation focused primarily on DPA.

### Cell Cycle Arrest and Mode of Cell Death

Flow cytometry was employed to investigate the impact of the complexes on the cell cycle of U87MG cells. DPA predominantly halted the cell cycle progression in the G1 phase, whereas SPA arrested it at both the G1 and G2 phases. Consistent with prior findings,<sup>32</sup> CDDP exhibited a cell cycle arrest effect in the G2 phase (Figure S16). The distinctive cell cycle arrest pattern induced by DPA contrasts significantly with that of CDDP,

strongly suggesting divergent mechanisms of action among them.

The mode of cell death was analyzed through an annexin V-FITC/propidium iodide (PI) double staining assay. Figure 3

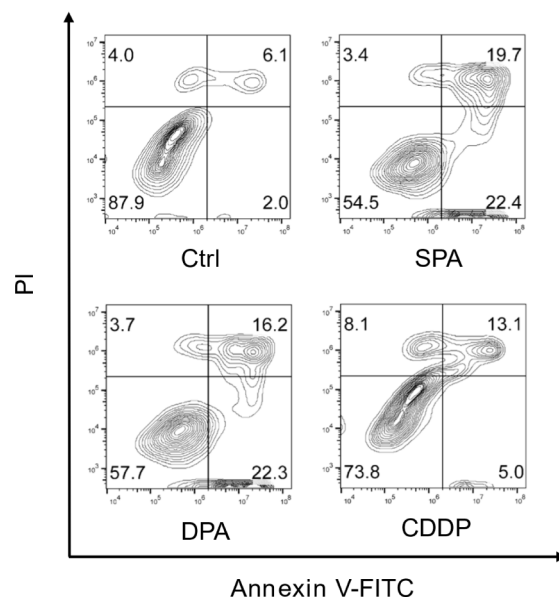


**Figure 3.** Apoptotic analysis of U87MG cells by flow cytometry after incubation with different complexes for 48 h.

illustrates that at 2 μM concentration, SPA and DPA prompted 22.4% and 22.3% of U87MG cells, respectively, to undergo early apoptosis, whereas CDDP only elicited early apoptosis in 5% of the cells. This observation underscores the potent proapoptotic efficacy of SPA and DPA and highlights their promising role in cancer therapy as compared to conventional agents like CDDP.

### Lipophilicity, Cellular Accumulation and DNA Platination

Lipophilicity significantly influences drug activity. SPA and DPA possess respective lipophilicities of  $1.37 \pm 0.08$  and  $2.09 \pm 0.20$ , determined by octanol–water partition coefficient ( $\log P_{O/W}$ ). This renders them more lipophilic than CDDP ( $\log P_{O/W} = -2.3$ ),<sup>33</sup> facilitating superior cell membrane penetration. Cellular Pt content, assessed via inductively coupled plasma mass spectrometry (ICP-MS) after 6-h incubation with CDDP, SPA, and DPA in U87MG cells, follows the sequence: DPA > SPA > CDDP, consistent with their lipophilicity and cytotoxicity (Figure 4A). Moreover, the capacity of SPA and DPA to bind nuclear DNA, a primary target of Pt complexes, was assessed post-treatment by extracting genomic DNA using a kit, followed by Pt quantification via ICP-MS. As shown in Figure 4B, the DNA platination follows an order of SPA > DPA ≈ CDDP, which is inconsistent with cellular uptake outcomes. It is conjectured that this inconsistency may stem from the sluggish reduction rate of DPA, thereby resulting in an insufficient release of Pt(II) species in cancer cells. DPA shows higher cytotoxicity despite similar DNA binding to CDDP, indicating non-DNA mechanisms at play.

### Inhibition of Ribosome Biogenesis

The biosynthesis of ribosomes initiates with the synthesis of precursor rRNA (47S pre-rRNA), marking the inception phase of the entire process. Subsequently, 47S pre-rRNA undergoes a series of intricate cleavage and post-transcriptional modification steps to mature into 5.8S, 18S, and 28S rRNA. These mature

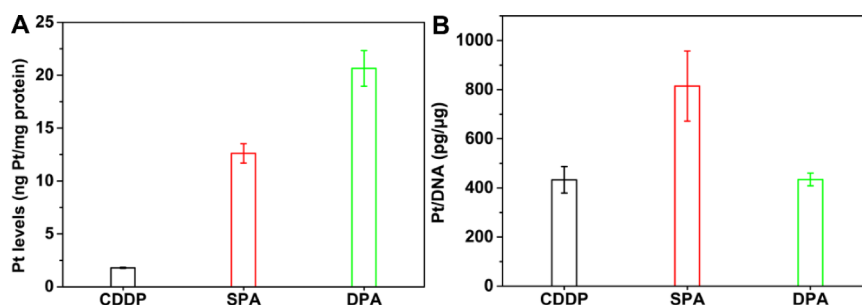


**Figure 4.** Cellular uptake of Pt (A) and platination of cellular DNA (B) in U87MG cells after exposure to CDDP, SPA and DPA for 6 h.

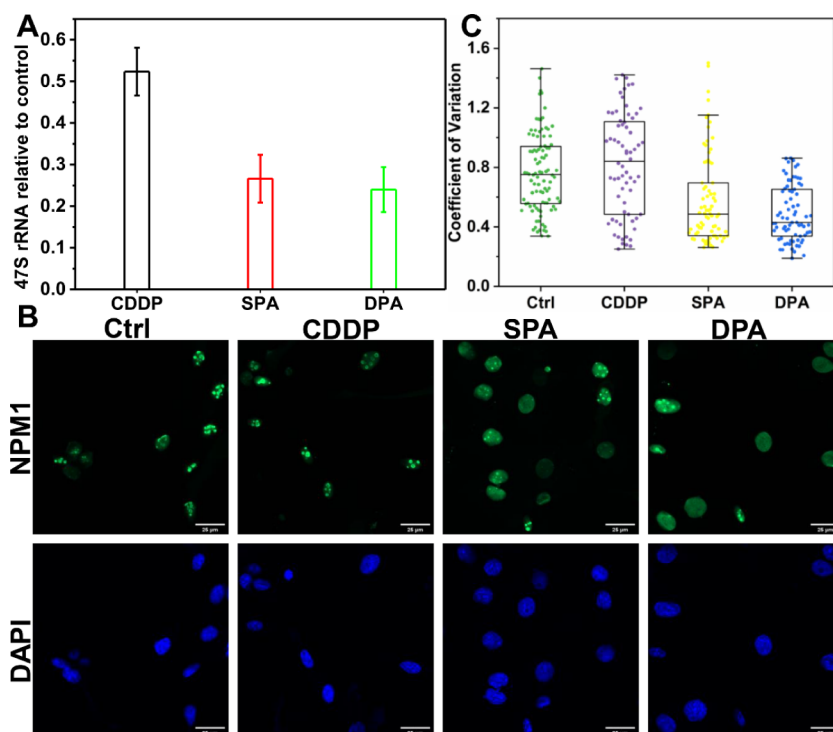


**Figure 5.** (A) The relative expression levels of 47S pre-rRNA and (B) NPM1 (green) relocalization in U87MG cells post drug treatment (5  $\mu$ M, 12 h). (C) Quantification of NPM1 relocalization induced by Pt complexes.

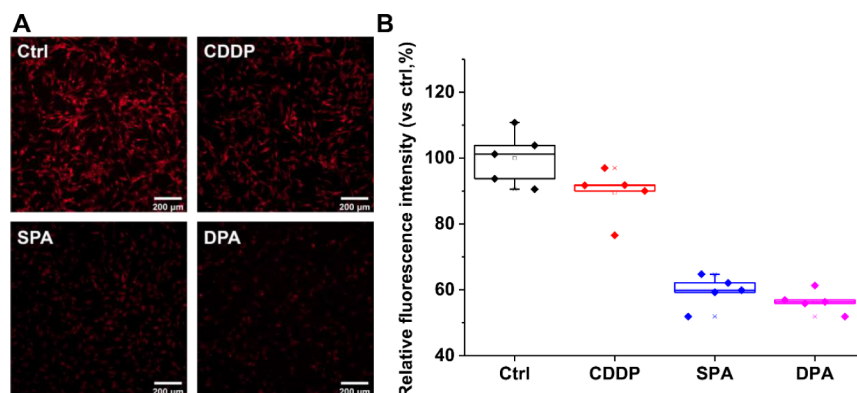


**Figure 6.** (A) Fluorescence images and (B) relative fluorescence intensity of newly synthesized peptides in U87MG cells post drug treatment.

rRNA molecules associate with ribosomal proteins and, through self-assembly processes, culminate in the formation of complete ribosomes.<sup>1</sup> Therefore, the synthesis of 47S pre-rRNA stands as a pivotal preliminary stage in ribosome biogenesis. To investigate the impact of compounds on this initial stage of ribosome biogenesis, we conducted relative quantitative analysis

of 47S pre-rRNA using fluorescence quantitative PCR (qPCR) technology. As shown in Figure 5A, the levels of 47S pre-rRNA in the CDDP-treated group exhibited a moderate decrease compared to the control group, possibly attributed to CDDP-induced rDNA damage. Interestingly, both SPA and DPA effectively suppressed the expression of 47S pre-rRNA in cells,

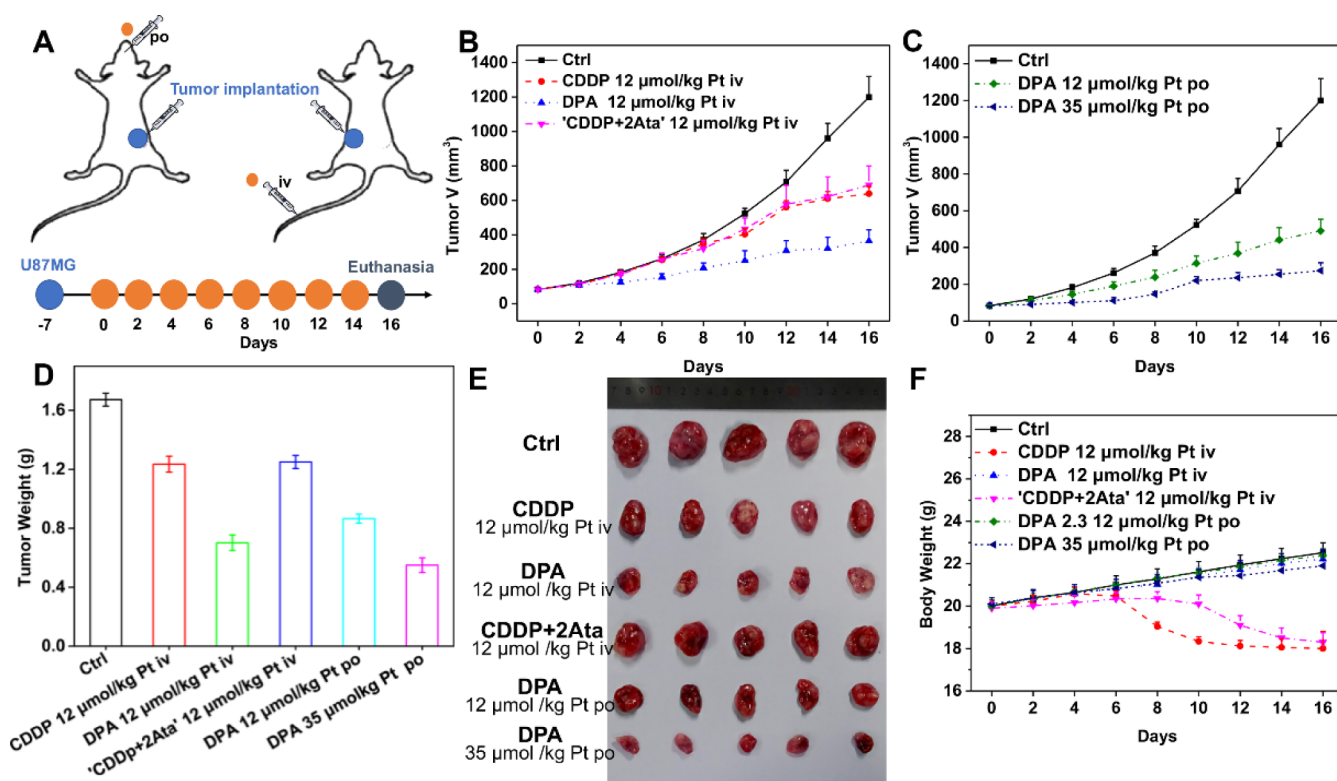


**Figure 7.** In vivo antitumor activity. (A) Schematic diagram of the in vivo antitumor experiment timeline. (B) Tumor growth after intravenous injection (iv) and (C) oral administration (po) are shown. (D) Weight, and (E) Images of tumor is shown. (F) Body weight during the treatment course is shown. “CDDP + 2Ata”: CDDP and Ata were administered separately at a 1:2 molar ratio (12 μmol/kg CDDP and 24 μmol/kg Ata).

surpassing the effect observed in the CDDP group. This suggests that SPA and DPA possess the capability to disrupt ribosome biogenesis. Such interference may further trigger nucleolar stress, wherein the NPM1 protein undergoes translocation from the nucleolus to the nucleoplasm, manifesting as a reduction in nucleolar presence and an increase in nucleoplasmic distribution, leading to a more diffuse cellular localization.<sup>34</sup> Immunofluorescence was employed to investigate the dispersion of NPM1 post drug treatment, as depicted in Figure 5B. While the control and CDDP groups displayed punctate NPM1 staining, SPA and DPA exhibited a dispersed pattern throughout the entire nuclear region, indicating significant nucleolar stress induction by the compounds. The degree of NPM1 redistribution was assessed by an image analysis protocol, quantifying the coefficient of variation (CV) of NPM1 intensity within individual cells. As depicted in Figure 5C, these compounds exhibit comparable trends.

### Inhibition of Protein Synthesis

Damages to ribosome biogenesis function result in a decrease in protein synthesis.<sup>3</sup> Hence, we employed alkyne-modified puromycin to detect nascent protein synthesis in drug-treated cells. Puromycin binds to nascent polypeptide chains and, through copper-catalyzed azide–alkyne cycloaddition (CuAAC) reaction, attaches a fluorescent label to the polypeptides. Reduction in fluorescence intensity using this method indicates a decrease in nascent protein synthesis over a relative period of time. As illustrated in Figure 6, cells treated with SPA and DPA exhibit a more pronounced decrease in fluorescence intensity compared to CDDP-treated cells, indicating a significant hindrance to the translation process. These above observations suggest that SPA and DPA effectively

interfere with ribosome biogenesis, thereby triggering nucleolar stress and ultimately leading to a marked reduction in nascent protein synthesis. Rapid proliferation of tumor cells necessitates substantial synthesis of nascent proteins; thus, compounds inhibiting nascent protein synthesis impair tumor cell function, leading to extensive cell death.

### Antitumor Activity in Subcutaneous Tumor Model

Xenograft models employing mice implanted with U87MG cells were utilized to assess the in vivo antitumor efficacy of DPA. The two administration routes, intravenous injection (iv) and oral administration (po), were employed, with dosing occurring once every 2 days for a total of eight administrations (Figure 7A). As shown in Figure 7B–E, strong inhibition of tumor growth was observed after the treatment. On day 16, the average tumor volume was  $1200 \pm 120$ ,  $639 \pm 42$  and  $689 \pm 110$  mm<sup>3</sup> for the control, CDDP and “CDDP + 2Ata” groups, respectively. Remarkably, DPA effectively suppressed the tumor growth. The average tumor volume in the DPA-treated groups after 16 d was  $365 \pm 64$  mm<sup>3</sup>, only reaching 30% of the control size (Figure 7B). Of greater significance, DPA demonstrates potent antitumor efficacy when administered orally, exhibiting a concentration-dependent relationship. In the high-dose group, the tumor volume after 16 days was  $274 \pm 43$  mm<sup>3</sup>, representing only 23% of the control group’s volume (Figure 7C). Similar trends were observed in tumor weight after 16 days (Figure 7D). Figure 7F indicates that regardless of whether administered intravenously or orally, DPA did not result in significant weight loss during the treatment course, unlike CDDP and “CDDP + 2Ata” groups, which showed noticeable declines in weight. This suggests that DPA exhibits low toxicity. The substantial in vivo

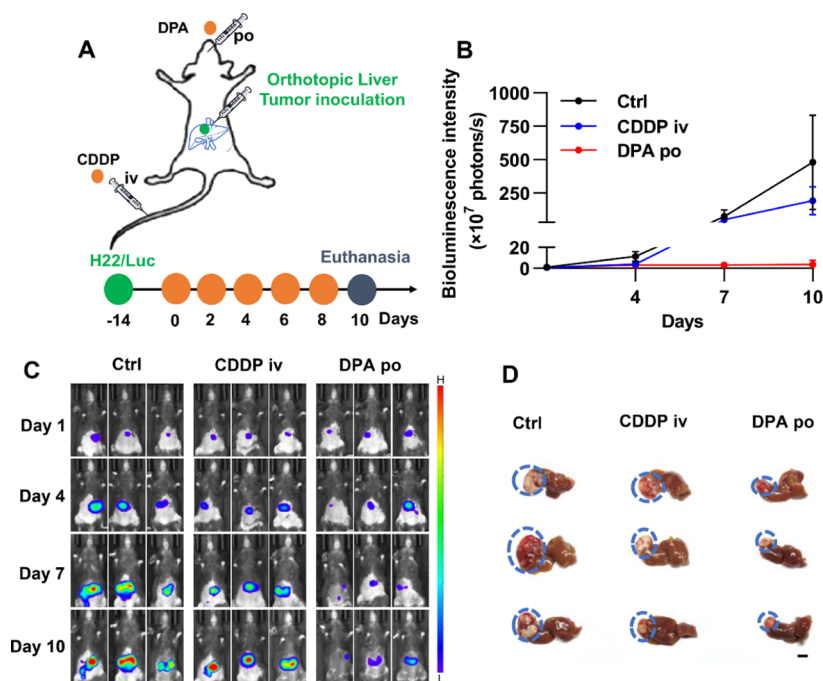


**Figure 8.** In vivo antitumor performance in orthotopic hepatic tumor mouse models. (A) Schematic diagram of the in vivo antitumor experiment timeline. (B) Intensity and (C) bioluminescence images of the orthotopic hepatic tumor mice on days 1, 4, 7, and 10. (D) Photographs of excised liver tissues bearing tumor from each treatment group at the end of treatment, scale bar = 0.5 cm.

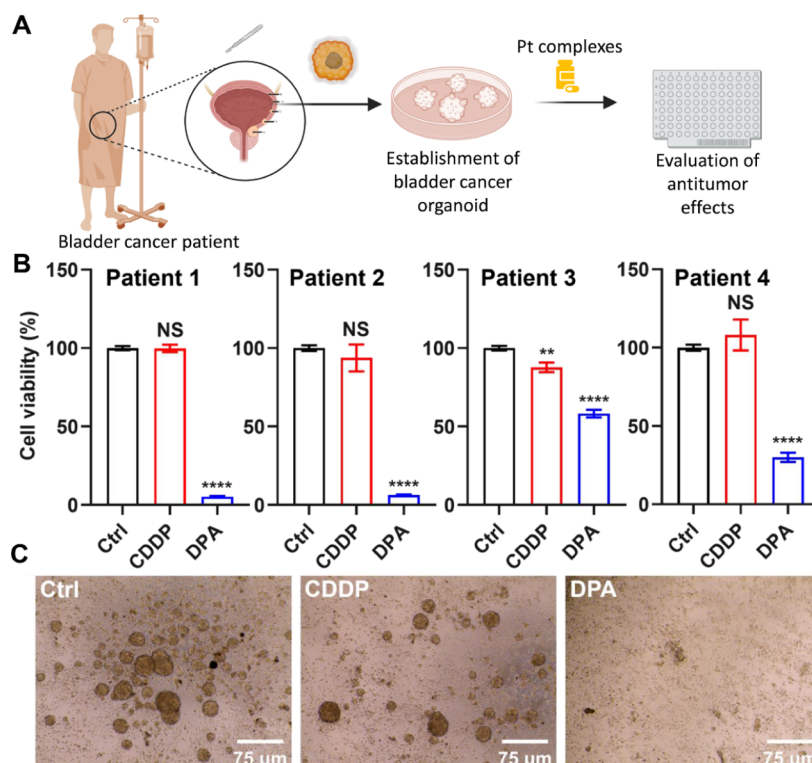


**Figure 9.** (A) Workflow of BCO culture and antitumor effect testing. (B) Cell viability of BCOs after the treatment of DPA and CDDP. NS: not significant, \*\* $p < 0.01$ , \*\*\*\* $p < 0.0001$ . (C) Bright-field microscopy images of drug-treated BCOs. Scale bar = 75  $\mu$ m.

antitumor efficacy coupled with minimal toxicity suggests the promising clinical applicability of DPA.

#### Antitumor Activity in Hepatic Orthotopic Tumor Model

In comparison to subcutaneous tumor models, orthotopic tumor models better replicate physiological conditions, enhancing drug efficacy assessment and facilitating metastasis

research.<sup>35</sup> After oral administration, drugs are initially transported to the liver via the portal venous system following intestinal absorption.<sup>36</sup> Therefore, we utilized the H22/Luc hepatic carcinoma in situ model to evaluate the oral antitumor activity of DPA. CDDP was administered intravenously, while DPA was administered orally every 2 days for a total of five doses

(Figure 8A). Results depicted in Figure 8B,D show that on the 10th day, tumors in the DPA treatment group were significantly smaller compared to the control and CDDP groups, indicating potent tumor suppression. This finding suggests a potential unique advantage of oral Pt(IV) complexes in gastrointestinal tumors, providing direction for its clinical application.

### Antitumor Activity in Patient-Derived Tumor Organoids

In the conventional approach to screening chemotherapy drugs, extensive libraries of small chemical compounds undergo rigorous evaluation against diverse cancer cell lines to pinpoint potential candidates with potent cytotoxic effects. Subsequently, promising compounds undergo further assessment in mouse models to gauge their *in vivo* efficacy, safety, and pharmacokinetics. Nevertheless, despite showing promise in mouse models, around 90% of preclinical drug candidates fail to advance to human clinical trials, underscoring a significant disparity between mouse and human models.<sup>37</sup> Recently, patient-derived tumor organoids (PDTOs) have emerged as a promising alternative. PDTOs faithfully replicate the complex structures, gene expressions, and molecular profiles of their parental tumors.<sup>38,39</sup> Previous studies have demonstrated the ability of PDTOs to accurately predict patient responses to various cancer treatments, including chemotherapy, targeted therapies, and combination regimens.<sup>40,41</sup> In previous studies, we established a bladder cancer patient-derived organoid (BCO) platform to assess the efficacy of Pt-based drugs.<sup>42</sup> Utilizing this platform, we evaluated the therapeutic effect of DPA. As depicted in Figure 9B,C, across four BCOs derived from different patients, DPA consistently exhibited significantly higher tumor-killing capacity than CDDP. However, variations in efficacy were observed among samples, likely attributable to individual differences. These findings demonstrate that DPA exhibits greater potency than CDDP and lay the groundwork for its clinical translation. It is noteworthy that at a concentration of 2  $\mu$ M, these BCOs show insensitivity to CDDP, suggesting a potential level of resistance. However, the high activity of DPA suggests its capability to overcome CDDP resistance effectively.

### CONCLUSION

Ribosomes, essential for protein synthesis, are regulated by a complex process of rRNA transcription, processing, and assembly with ribosomal protein.<sup>1,3</sup> Dysregulation of ribosome biogenesis is implicated in diseases, notably cancer, where upregulation supports rapid cell proliferation.<sup>1,3</sup> Targeting ribosome biogenesis thus emerges as a promising cancer therapy strategy. Pt(II) complexes, such as oxaliplatin and its derivatives, traditionally known for inducing DNA damage, also induce ribosome biogenesis stress.<sup>11,12</sup> However, there is a scarcity of reports documenting the targeting of ribosomes by Pt(IV) derivatives. Here, we report two Pt(IV) prodrugs, SPA and DPA, derived from CDDP, demonstrating their effective cellular uptake and binding to nuclear DNA, subsequently inducing apoptosis. Further investigations reveal that SPA and DPA effectively suppress the expression of 47s pre-RNA, a critical step in ribosome biogenesis,<sup>1</sup> leading to the dispersion of nucleolar protein NPM1, triggering nucleolar stress, and ultimately inhibiting the generation of new proteins in tumor cells. Remarkably, DPA exhibits significantly higher cytotoxicity and *in vivo* antitumor efficacy compared to CDDP, with lower systemic toxicity. Furthermore, the oral efficacy of DPA remains intact, promising clinical feasibility. In clinically relevant models (orthotopic liver cancer-bearing mice and patient-derived

bladder cancer organoids), DPA retains its efficacy, surpassing CDDP markedly, hinting at substantial clinical translational potential. The potent activity and unique mechanism of action of DPA not only broaden the diversity of Pt drug mechanisms but also provide a novel direction for designing next-generation metal-based therapeutics.

In addition, Pt(IV) prodrugs are recognized candidates for oral administration, with cisplatin-sensitive cancers such as prostate, lung, and ovarian cancers being primary indications for satraplatin clinical trials.<sup>19</sup> Given the requirement for oral drugs to pass through the digestive system, we explored the therapeutic effects of DPA in an orthotopic liver cancer model and found substantial efficacy. This suggests that oral Pt(IV) prodrugs may be particularly suitable for digestive system tumors, which often exhibit limited sensitivity to cisplatin. Despite incomplete understanding of DPA's tissue distribution within the digestive system, this pioneering investigation provides valuable insights for applied research and the selection of clinical indications of oral Pt(IV) complexes. Overall, this study highlights the effectiveness of targeting ribosomes against tumors, while also illuminating the remarkable prowess of metallodrugs, especially Pt(IV) prodrugs, in this endeavor. Moving forward, we are systematically evaluating the drug metabolism, pharmacokinetics, and toxicity profiles of compounds, and further optimizing molecules to enhance the drug-like properties with the aim of realizing their translational potential.

### ASSOCIATED CONTENT

#### Data Availability Statement

The data that support the findings of this study are available in the Supporting Information of this article.

#### Supporting Information

The Supporting Information is available free of charge at <https://pubs.acs.org/doi/10.1021/jacsau.4c00652>.

Additional experimental details, materials, and methods, including photographs of experimental setup (PDF)

### AUTHOR INFORMATION

#### Corresponding Authors

**Shuren Zhang** – School of Chemistry and Chemical Engineering, Chemistry and Biomedicine Innovation Center (ChemBIC), State Key Laboratory of Coordination Chemistry, Nanjing University, Nanjing 210023, PR China; [orcid.org/0000-0002-9833-7423](https://orcid.org/0000-0002-9833-7423); Email: [zhangshuren@nju.edu.cn](mailto:zhangshuren@nju.edu.cn)

**Zijian Guo** – School of Chemistry and Chemical Engineering, Chemistry and Biomedicine Innovation Center (ChemBIC), State Key Laboratory of Coordination Chemistry, Nanjing University, Nanjing 210023, PR China; [orcid.org/0000-0003-4986-9308](https://orcid.org/0000-0003-4986-9308); Email: [zguo@nju.edu.cn](mailto:zguo@nju.edu.cn)

#### Authors

**Dongfan Song** – School of Chemistry and Chemical Engineering, Chemistry and Biomedicine Innovation Center (ChemBIC), State Key Laboratory of Coordination Chemistry, Nanjing University, Nanjing 210023, PR China

**Xiaoyu Wang** – School of Chemistry and Chemical Engineering, Chemistry and Biomedicine Innovation Center (ChemBIC), State Key Laboratory of Coordination Chemistry, Nanjing University, Nanjing 210023, PR China

Zihan Zhao – Department of Urology, Nanjing Drum Tower Hospital, Affiliated Hospital of Medical School, Nanjing University, Nanjing 210093, PR China; [orcid.org/0000-0002-3391-1041](https://orcid.org/0000-0002-3391-1041)

Rong Yang – Department of Urology, Nanjing Drum Tower Hospital, Affiliated Hospital of Medical School, Nanjing University, Nanjing 210093, PR China

Complete contact information is available at:  
<https://pubs.acs.org/10.1021/jacsau.4c00652>

### Author Contributions

§D.S., X.W., and Z.Z. contributed equally to this work.

### Notes

The authors declare no competing financial interest.

### ACKNOWLEDGMENTS

We thank the National Natural Science Foundation of China (22293050, 22293051, 22107047, 92153303 and 91953201), Natural Science Foundation of Jiangsu Province (BK20232020), and Excellent Research Program of Nanjing University (ZYJH004).

### REFERENCES

- (1) Pelletier, J.; Thomas, G.; Volarevic, S. Ribosome biogenesis in cancer: new players and therapeutic avenues. *Nat. Rev. Cancer* **2018**, *18*, 51–63.
- (2) Elhamamsy, A. R.; Metge, B. J.; Alsheikh, H. A.; Shevde, L. A.; Samant, R. S. Ribosome Biogenesis: A Central Player in Cancer Metastasis and Therapeutic Resistance. *Cancer Res.* **2022**, *82* (13), 2344–2353.
- (3) Jiao, L.; Liu, Y.; Yu, X.-Y.; Pan, X.; Zhang, Y.; Tu, J.; Song, Y.-H.; Li, Y. Ribosome biogenesis in disease: new players and therapeutic targets. *Signal Transduction Targeted Ther.* **2023**, *8* (1), 15.
- (4) Catez, F.; Venezia, N. D.; Marcel, V.; Zorbas, C.; Lafontaine, D. L. J.; Diaz, J.-J. Ribosome biogenesis: An emerging druggable pathway for cancer therapeutics. *Biochem. Pharmacol.* **2019**, *159*, 74–81.
- (5) Lindström, M. S.; Bartek, J.; Maya-Mendoza, A. p53 at the crossroad of DNA replication and ribosome biogenesis stress pathways. *Cell Death Differ.* **2022**, *29* (5), 972–982.
- (6) Ogawa, L. M.; Baserga, S. J. Crosstalk between the nucleolus and the DNA damage response. *Mol. Biosyst.* **2017**, *13* (3), 443–455.
- (7) Boon, N. J.; Oliveira, R. A.; Körner, P.-R.; Kochavi, A.; Mertens, S.; Malka, Y.; Voogd, R.; Horst, S. E. M. V. D.; Huisman, M. A.; Smabers, L. P.; et al. DNA damage induces p53-independent apoptosis through ribosome stalling. *Science* **2024**, *384* (6697), 785–792.
- (8) Johnstone, T. C.; Suntharalingam, K.; Lippard, S. J. The Next Generation of Platinum Drugs: Targeted Pt(II) Agents, Nanoparticle Delivery, and Pt(IV) Prodrugs. *Chem. Rev.* **2016**, *116* (5), 3436–3486.
- (9) Casini, A.; Pöthig, A. Metals in Cancer Research: Beyond Platinum Metalloproteins. *ACS Cent. Sci.* **2024**, *10* (2), 242–250.
- (10) Jung, Y.; Lippard, S. J. Direct Cellular Responses to Platinum-Induced DNA Damage. *Chem. Rev.* **2007**, *107*, 1387–1407.
- (11) Bruno, P. M.; Liu, Y.; Park, G. Y.; Murai, J.; Koch, C. E.; Eisen, T. J.; Pritchard, J. R.; Pommier, Y.; Lippard, S. J.; Hemann, M. T. A subset of platinum-containing chemotherapeutic agents kills cells by inducing ribosome biogenesis stress. *Nat. Med.* **2017**, *23* (4), 461–471.
- (12) Sutton, E. C.; McDevitt, C. E.; Prochnau, J. Y.; Yglesias, M. V.; Mroz, A. M.; Yang, M. C.; Cunningham, R. M.; Hendon, C. H.; DeRose, V. J. Nucleolar Stress Induction by Oxaliplatin and Derivatives. *J. Am. Chem. Soc.* **2019**, *141* (46), 18411–18415.
- (13) Melnikov, S. V.; Söll, D.; Steitz, T. A.; Polikanov, Y. S. Insights into RNA binding by the anticancer drug cisplatin from the crystal structure of cisplatin-modified ribosome. *Nucleic Acids Res.* **2016**, *44* (10), 4978–4987.
- (14) Jordan, P.; Carmo-Fonseca, M. Cisplatin inhibits synthesis of ribosomal RNA in vivo. *Nucleic Acids Res.* **1998**, *26*, 2831–2836.
- (15) Wang, X.; Guo, Z. Targeting and delivery of platinum-based anticancer drugs. *Chem. Soc. Rev.* **2013**, *42* (1), 202–224.
- (16) Wang, X.; Wang, X.; Jin, S.; Muhammad, N.; Guo, Z. Stimuli-Responsive Therapeutic Metalloproteins. *Chem. Rev.* **2019**, *119*, 1138–1192.
- (17) Zhang, S.; Wang, X.; Guo, Z. Rational design of anticancer platinum(IV) prodrugs. *Adv. Inorg. Chem.* **2020**, *75*, 149–182.
- (18) Kenny, R. G.; Marmion, C. J. Toward Multi-Targeted Platinum and Ruthenium Drugs—A New Paradigm in Cancer Drug Treatment Regimens? *Chem. Rev.* **2019**, *119*, 1058–1137.
- (19) Choy, H. Satraplatin: an orally available platinum analog for the treatment of cancer. *Expert Rev. Anticancer Ther.* **2006**, *6* (7), 973–982.
- (20) Wang, Z.; Xu, Z.; Zhu, G. A Platinum(IV) Anticancer Prodrug Targeting Nucleotide Excision Repair To Overcome Cisplatin Resistance. *Angew. Chem., Int. Ed.* **2016**, *55* (50), 15564–15568.
- (21) Karges, J.; Yempala, T.; Tharaud, M.; Gibson, D.; Gasser, G. A Multi-action and Multi-target Ru(II)-Pt(IV) Conjugate Combining Cancer-Activated Chemotherapy and Photodynamic Therapy to Overcome Drug Resistant Cancers. *Angew. Chem., Int. Ed.* **2020**, *59* (18), 7069–7075.
- (22) Yang, T.; Zhang, S.; Yuan, H.; Wang, Y.; Cai, L.; Chen, H.; Wang, X.; Song, D.; Wang, X.; Guo, Z.; Wang, X. Platinum-Based TREM2 Inhibitor Suppresses Tumors by Remodeling the Immunosuppressive Microenvironment. *Angew. Chem., Int. Ed.* **2023**, *62* (2), No. e202213337.
- (23) Babak, M. V.; Zhi, Y.; Czarny, B.; Toh, T. B.; Hooi, L.; Chow, E. K.-H.; Ang, W. H.; Gibson, D.; Pastorin, G. Dual-targeting Dual-action Platinum(IV) Platform for Enhanced Anticancer Activity and Reduced Nephrotoxicity. *Angew. Chem., Int. Ed.* **2019**, *58*, 8109–8114.
- (24) Zhang, S.; Song, D.; Yu, W.; Li, J.; Wang, X.; Li, Y.; Zhao, Z.; Xue, Q.; Zhao, J.; Li, J. P.; Guo, Z. Combining cisplatin and a STING agonist into one molecule for metalloimmunotherapy of cancer. *Natl. Sci. Rev.* **2024**, *11* (1), nwae020.
- (25) Kalathil, A. A.; Guin, S.; Ashokan, A.; Basu, U.; Surnar, B.; Delma, K. S.; Lima, L. M.; Kryvenko, O. N.; Dhar, S. New Pathway for Cisplatin Prodrug to Utilize Metabolic Substrate Preference to Overcome Cancer Intrinsic Resistance. *ACS Cent. Sci.* **2023**, *9* (7), 1297–1312.
- (26) Roy, B.; Friesen, W. J.; Tomizawa, Y.; Leszyk, J. D.; Zhuo, J.; Johnson, B.; Dakka, J.; Trotta, C. R.; Xue, X.; Mutyam, V.; Keeling, K. M.; Mobley, J. A.; Rowe, S. M.; Bedwell, D. M.; Welch, E. M.; Jacobson, A. Ataluren stimulates ribosomal selection of near-cognate tRNAs to promote nonsense suppression. *Proc. Natl. Acad. Sci. U.S.A.* **2016**, *113*, 12508–12513.
- (27) Raymer, B.; Bhattacharya, S. K. Lead-like Drugs: A Perspective. *J. Med. Chem.* **2018**, *61* (23), 10375–10384.
- (28) Michorowska, S. Ataluren—Promising Therapeutic Premature Termination Codon Readthrough Frontrunner. *Pharmaceuticals* **2021**, *14* (8), 785.
- (29) Pathak, R. K.; Dhar, S. Unique Use of Alkylation for Chemo-Redox Activity by a Pt<sup>IV</sup> Prodrug. *Chem.-Eur. J.* **2016**, *22*, 3029–3036.
- (30) Wang, X.; Song, D.; Nie, J.; Zou, L.; Wang, W.; Zhang, S.; Guo, Z. Overcoming Cancer Chemoresistance Through Chromatin Compaction with Orally Platinum-Based ACLY Inhibitors. *CCS Chem.* **2024**, *1*.
- (31) Wang, Z.; Deng, Z.; Zhu, G. Emerging platinum(IV) prodrugs to combat cisplatin resistance: from isolated cancer cells to tumor microenvironment. *Dalton Trans.* **2019**, *48*, 2536–2544.
- (32) Zheng, Y. R.; Suntharalingam, K.; Johnstone, T. C.; Yoo, H.; Lin, W.; Brooks, J. G.; Lippard, S. J. Pt(IV) prodrugs designed to bind non-covalently to human serum albumin for drug delivery. *J. Am. Chem. Soc.* **2014**, *136* (24), 8790–8798.
- (33) Oldfield, S. P.; H, M. D.; Platts, J. A. Calculation of Lipophilicity of a Large, Diverse Dataset of Anticancer Platinum Complexes and the Relation to Cellular Uptake. *J. Med. Chem.* **2007**, *50* (21), 5227–5237.
- (34) Yang, K.; Wang, M.; Zhao, Y.; Sun, X.; Yang, Y.; Li, X.; Zhou, A.; Chu, H.; Zhou, H.; Xu, J.; Wu, M.; Yang, J.; Yi, J. A redox mechanism underlying nucleolar stress sensing by nucleophosmin. *Nat. Commun.* **2016**, *7* (1), 13599.

- (35) Killion, J. J.; Radinsky, R.; Fidler, I. J. Orthotopic models are necessary to predict therapy of transplantable tumors in mice. *Cancer Metast. Rev.* **1998**, *17*, 279–284.
- (36) Gibaldi, M.; Perrier, D. Route of Administration and Drug Disposition. *Drug Metabol. Rev.* **1975**, *3* (1), 185–199.
- (37) Sharpless, N. E.; DePinho, R. A. The mighty mouse: genetically engineered mouse models in cancer drug development. *Nat. Rev. Drug Discovery* **2006**, *5* (9), 741–754.
- (38) Drost, J.; Clevers, H. Organoids in cancer research. *Nat. Rev. Cancer* **2018**, *18* (7), 407–418.
- (39) Kim, J.; Koo, B.-K.; Knoblich, J. A. Human organoids: model systems for human biology and medicine. *Nat. Rev. Mol. Cell Bio.* **2020**, *21* (10), 571–584.
- (40) Pasch, C. A.; Favreau, P. F.; Yueh, A. E.; Babiarz, C. P.; Gillette, A. A.; Sharick, J. T.; Karim, M. R.; Nickel, K. P.; DeZeeuw, A. K.; Sprackling, C. M.; Emmerich, P. B.; DeStefanis, R. A.; Pitera, R. T.; Payne, S. N.; Korkos, D. P.; Clipson, L.; Walsh, C. M.; Miller, D.; Carchman, E. H.; Burkard, M. E.; Lemmon, K. K.; Matkowskyj, K. A.; Newton, M. A.; Ong, I. M.; Bassetti, M. F.; Kimple, R. J.; Skala, M. C.; Deming, D. A. Patient-Derived Cancer Organoid Cultures to Predict Sensitivity to Chemotherapy and Radiation. *Clin. Cancer Res.* **2019**, *25* (17), 5376–5387.
- (41) Skala, M. C.; Deming, D. A.; Kratz, J. D. Technologies to Assess Drug Response and Heterogeneity in Patient-Derived Cancer Organoids. *Annu. Rev. Biomed. Eng.* **2022**, *24* (1), 157–177.
- (42) Zhao, Z.; Zhang, S.; Jiang, N.; Zhu, W.; Song, D.; Liu, S.; Yu, W.; Bai, Y.; Zhang, Y.; Wang, X.; Zhong, X.; Guo, H.; Guo, Z.; Yang, R.; Li, J. P. Patient-derived Immunocompetent Tumor Organoids: A Platform for Chemotherapy Evaluation in the Context of T-cell Recognition\*\*. *Angew. Chem., Int. Ed.* **2024**, *63* (9), No. e202317613.